Journal of Hazardous Materials 186 (2011) 629–635

Contents lists available at ScienceDirect

Journal of Hazardous Materials

journal homepage: www.elsevier.com/locate/jhazmat

Kinetic and regeneration studies of photocatalytic magnetic separable beads for chromium (VI) reduction under sunlight

Ani Idris[a,*], Nursia Hassan[a], Roslina Rashid[a], Audrey-Flore Ngomsik[b]

[a] Department of Bioprocess Engineering, Faculty of Chemical and Natural Resource Engineering, Universiti Teknologi Malaysia, 81310 Skudai, Johor, Malaysia
[b] Green Chemistry & Processes for Sustainable Development, Université de Reims Champagne Ardenne, Bâtiment 13 Recherche, 57 bis rue Pierre Taittinger, 51096 Reims Cedex, France

ARTICLE INFO

Article history:
Received 11 April 2010
Received in revised form 2 November 2010
Accepted 11 November 2010
Available online 2 December 2010

Keywords:
Photocatalyst
Magnetic beads
Magnetic nanoparticles
Maghemite
Langmuir–Hinshelwood model
Regeneration

ABSTRACT

Physical adsorption and photocatalytic reduction of Cr(VI) in magnetic separable beads were investigated. In order to elucidate the kinetics of photocatalytic process, operating parameters such as catalyst dosage and the initial concentration were examined in detail. It was observed that the reduction rate of Cr(VI) increased with an increase in the catalyst loading, as this translated into an increase in the number of available active sites. Critical scrutiny of the percentage of the initial reduction rate versus time at various initial concentration of Cr(VI) revealed that the rate of substrate conversion decreased as the initial concentration increased. The kinetic analysis of the photoreduction showed that the removal of Cr(VI) satisfactory obeyed the pseudo first-order kinetic according to the Langmuir–Hinshelwood (L–H) model and the absorption of Cr(VI) on the magnetic beads surfaces was the controlling step in the entire reduction process. Furthermore, desorption experiments by elution of the loaded gels with sodium hydroxide indicated that the magnetic photocatalyst beads could be reused without significant losses of their initial properties even after 3 adsorption–desorption cycles.

1. Introduction

Over the decade, chromium pollution in water has become a concern due to its extensive use in chemical industries for electroplating, leather tanning or paint processes. In general, hexavalent form of chromium is 100 times more acutely toxic than the trivalent form [1] and thus, exposure to Cr(VI) has been demonstrated to cause cancer in the digestive tract and lungs, epigastria pain and nausea [2] whereas Cr(III) is an essential nutrient at trace levels. Hence, increasing awareness has been growing rapidly worldwide and one of the offshoots is the treatment and removal of this toxic material from such effluents to a permissible limit before discharging them into streams and rivers. The Occupational Safety and Health Administration (OSHA) has set the maximum contaminant level (MCL) for Cr(VI) to be 0.005 mg/m^3 while for Cr(III) 0.5 mg/m^3 for an 8 h workday, 40 h workweek [3]. According to the Malaysian Standard B, the permissible discharge limit for Cr(VI) is 0.05 mg/L. In order to comply with this limit, it is imperative for industries to decrease the chromium in their effluents to an acceptable level. The preferred treatment of Cr(VI) is the reduction to Cr(III) and the subsequent hydroxide precipitation of Cr(III).

The complexities lay primarily with issues of technology selection, integration and practical constraint such as cost. In water and wastewater treatment technologies, photocatalytic remediation was found to be suitable for aqueous solutions that contain organic compounds and reducible toxic metal ions because it was found that the photocatalytic oxidation of organics and reduction of metals are synergistic [4,5]. This observation was explained in terms of a closed redox cycle whereby the organics are destroyed by photocatalytic oxidation while the metals are removed by reduction. In principle, photocatalyst are able to convert pollutants into less toxic forms. In contrast to the current treatment methods where adsorption is mostly used, the contaminants are merely concentrated by the chemicals present, whereby transferring them to the adsorbent but they do not convert them into less toxic wastes [6].

Titanium dioxide as the most common heterogeneous photocatalyst used in the photocatalysis process shows higher efficiency for the reduction and oxidation of organic and inorganic substrates [5,7]. However certain limitation exists when using titanium dioxide, TiO_2, in photocatalytic reaction. For example, due to the small size, (about 2–10 nm) TiO_2 aggregates rapidly in suspension losing its surface area as well as the catalytic efficiency. Moreover titania is only active with UV light or radiation with wavelength approximately below 387 nm, which makes it unavailable for wider applications. Furthermore, TiO_2 particles cannot be used as a photocatalyst in a commercial suspension system due

* Corresponding author. Tel.: +07 5535603; fax: +07 5581463.
E-mail address: ani@fkkksa.utm.my (A. Idris).

0304-3894/$ – see front matter © 2010 Elsevier B.V. All rights reserved.
doi:10.1016/j.jhazmat.2010.11.101

to the high cost involved when separating them from the treated water [8].

In recent years, zero-valent iron (Fe^0) nanoparticles have received much attention for their potential application for reduction of hexavalent chromium or Cr(VI) due to their high surface area and reactivity [9]. However, zero-valent iron nanoparticles tend to agglomerate rapidly in the range of sub-micron scale and react quickly with the surrounding media such as dissolved oxygen and water resulting in significant loss in reactivity [10]. Thus, there is a need to explore more suitable materials for transforming toxic transition metals ion into non-toxic substances.

The synthesis of nanostructure magnetic materials has become a particularly important area of research and is attracting a growing interest because of its potential applications in the field of biomedical and water remediation. In biomedical applications magnetic nanoparticle technology has achieved widespread usage in drug delivery, magnetic resonance imaging, tissue repair, hyperthermia and diagnostics. Recently, it was used in water remediation as catalysts [11] and adsorbents [12,13] for the removal of heavy metals in waste effluents due to its high surface area, porous structure, and highly active surface sites.

Ngomsik et al. [14] have used magnetic alginate microcapsule containing an extractant of Cyanex 272 to remove the heavy metal nickel (II) from water. In another study [2], bio-functional magnetic beads were prepared using PVA alginate, powdered Rhizopus cohnii and Fe_3O_4 particles coated with alginate and polyvinyl alcohol (PVA) as adsorbent for the Cr(VI) removal from water. Previously Hu et al. [12] synthesized maghemite nanoparticles and used it as an adsorbent to remove Cr(VI). However in all these studies [2,12,14] the magnetic alginate microcapsules were mostly used as adsorbents, whereby the adsorption process just transfers pollutants from one phase to another rather than eliminating them from the environment.

Recently, it was reported for the first time, that magnetic beads can be used as photocatalyst for Cr(VI) removal [11]. In the method mentioned the maghemite nanoparticles (γ-Fe_2O_3) was entrapped in the matrix of sodium alginate thus forming magnetic separable beads capable of reducing Cr(VI) to Cr(III). The sunlight driven photocatalyst are capable of reducing 100% of the Cr(VI) to Cr(III) in a very short period of 50 min. However when the magnetic beads were placed away from the sunlight only 10% of the Cr(VI) were reduced to Cr(III) due to the adsorption of Cr(VI) onto the surface of the beads. This study revealed that synthesized magnetic beads were sunlight driven photocatalyst [11]. In addition, the advantage of using the magnetic beads in removing Cr(VI) is that no secondary waste treatment is required. The harmless Cr(III) can be released to the environment if they are within the required limits. Furthermore, the magnetism of the photocatalyst beads which arises from the nanostructure particles of γ-Fe_2O_3 allows for their facile recovery from the treated water by simple magnetic force without the need for further downstream treatment process and thus reduces cost. Also the possibility of recycling and reusing the photocatalyst beads offers an attractive alternative.

In the previous study [11], only the influence of pH was studied and found to play an appreciable role in influencing photoreduction of Cr(VI) to Cr(III). In this paper other process parameters such as the initial concentration of the substrate and catalyst loading including kinetic models involve in the photoreduction of Cr(VI) to Cr(III) are investigated. In addition, the regeneration study was performed making it more commercially viable as once separated, this photocatalyst can be reused because of its regenerative property under photocatalytic reaction. The ability of the photocatalyst to be reused is an essential practical aspect of the cost effectiveness in every related process [15].

2. Materials and methods

2.1. Materials

Iron (II) chloride ($FeCl_2$, 98%) and Iron (III) chloride solution ($FeCl_3$, 45%) were purchased from Sigma Aldrich and Riedel-de Haen respectively. Hydrochloric acid (HCl, 37%), nitric acid (HNO_3, 65%, v/v), acetone, potassium dichromate ($K_2Cr_2O_7$, 99.9%) and 1,5-diphenylcarbazide (DPC, 98%) were purchased from QReC and ammonia solution (NH_3, 25%, w/v) was provided by Merck. Sodium alginate was obtained from Fluka. All the above materials were used without further purification. Distilled, deionized water was used throughout this work.

2.2. Preparation of magnetic maghemite nanoparticles

The preparation of the magnetic maghemite nanoparticles has been described elsewhere [16]. The magnetic material used was ferrofluid composed of maghemite (γ-Fe_2O_3) nanoparticles coated by citrate ions and dispersed in an aqueous solution. Particles were synthesized by co precipitation of a stoichiometric mixture of ferrous and ferric chlorides in an ammonium hydroxide solution. The magnetite (Fe_3O_4) precipitate obtained was acidified by nitric acid and oxidized into maghemite (γ-Fe_2O_3) at 90 °C with iron (III) nitrate. To obtain a stable magnetic dispersion compatible with an alginate gel (neutral medium), particles were coated by citrate anions. After precipitation with acetone, coated particles were dispersed in water to obtain a stable ferrofluid with a pH of 7. The characterization of the maghemite nanoparticles was described in our previous paper [11].

2.3. Preparation of the magnetically separable photocatalyst beads

Preparation of the magnetic photocatalyst beads involved the entrapment of γ-Fe_2O_3 particles in the matrix of sodium alginate, followed by ionic polymerization. The method of preparation was reported in a previous study [11] where approximately 300 ml of the precursor solution was prepared by mixing 8.0 g of sodium alginate powder and 50.0 ml of ferrofluid in distilled water. In order to ensure homogeneity the mixture was continuously stirred with a mechanical stirrer for 1 h. The precursor suspension was then added dropwise into the 0.5 M calcium chloride solution. In order to draw the beads away from the dropping zone a magnet was placed under the calcium chloride solution. The beads were kept in the calcium chloride solution overnight, so as to permit them to cure and also ensure that the gelation reaction time was sufficient for the whole volume of the beads. The magnetic nanoparticles were prevented from leaching out of the beads by the protective membrane formed by the instantaneous crosslinking of the interfacial alginate chains by calcium ions. The beads were washed several times with distilled water and stored in a distilled water bath to ensure the removal of all unbound calcium [11]. In order to avert the collapse of the internal structure, the beads were stored wet. The JEOL JSM-6701F field emission scanning electron microscopy (FESEM) was used to capture images of magnetic beads at different states. The bead sample was sliced before FESEM analysis. The FESEM equipment was also equipped with an energy-dispersive X-ray (EDX) system so that EDX could be used to determine the elemental composition at selected spots of the sample surface.

2.4. Apparatus

The photocatalytic activity of magnetic beads was evaluated by photoreduction of hexavalent chromium in acidic solution. All photocatalytic reaction was performed under sunlight irradiation and

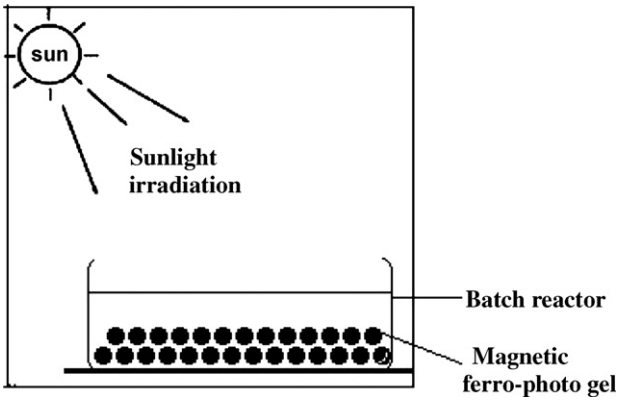

Fig. 1. Experimental set-up for the photocatalytic reduction of hexavalent chromium.

100 ml of Cr(VI) was mixed with prepared amounts of magnetic photocatalyst beads in a beaker as depicted in Fig. 1. The Cr(VI) solution was analysed by taking 5 ml sample every 10 min during the entire irradiation treatment.

2.5. Photocatalytic reactions

The photocatalytic reduction of hexavalent chromium was performed taking 100 ml of 50 mg/L Cr(VI) solution in 100 ml Pyrex flask and contacted with 10.0 g (wet weight) of magnetically separable beads. The pH of the dispersion was adjusted to 1–2 by addition of hydrochloric acid (HCl). pH 1–2 was chosen based on our previous report [11]. The solutions were exposed to sunlight. All the experiments were performed during sunny days from 10.00 a.m. to 14.00 p.m and in triplicates to evaluate repeatability. After irradiation the suspension was collected and the Cr(VI) concentration was determined colorimetrically at 540 nm using the UV–vis spectrophotometer (Shimadzu, Japan)

2.6. Effect of initial concentration of Cr(VI) on photoreduction kinetics

In order to study the influence of initial concentration on the photocatalytic activity, the initial Cr(VI) concentration was varied at 25, 50, 75, 100, 125 and 150 mg/L, and irradiated for 100 min. The catalyst concentration and pH were maintained at 16% (v/v) and 1.0 respectively based on our previous study [11] which revealed that Cr(VI) removal was highest at these mentioned conditions. Sampling was performed by taking 5 ml sample every 10 min during the whole irradiation process.

2.7. Effect of photocatalyst dosage on photocatalytic activity kinetics

The effect of photo catalyst dosage on Cr(VI) reduction was investigated by varying the dosage of ferrofluid to 8%, 16% and 25% (v/v). The initial concentration of Cr(VI) was fixed at 50 mg/L. The pH was kept at 1. The 8% (v/v) ferrofluid dosage was prepared by mixing 8.0 g of sodium alginate powder and 25.0 ml of ferrofluid in distilled water with a total volume of 300 ml. The other ferrofluid dosages were prepared in the same manner except for the ferrofliud volume which was varied.

2.8. Recyclability

The used magnetic beads was regenerated by washing with 0.01 M NaOH for 1 h and reused as in Section 2.4. The initial concentration of Cr(VI) used was varied at 25, 50 and 75 mg/L. The concentration of catalyst was fixed at 16% (v/v). The whole process was repeated several times to investigate the magnetic beads regeneration properties and the number of times they can be reused.

2.9. Analysis

Chromium (VI) reduction was determined colorimetrically at 540 nm using the diphenylcarbazide (DPC) method with a detection limit of 5 μg/L. Sample, 1 ml, was mixed with 9 ml of 0.2 M H_2SO_4 in a 10 ml volumetric flask. Subsequently 0.2 ml of freshly prepared 0.25% (w/v) DPC in acetone was added to the volumetric flask. After vortexing the mixture for about 15–30 s it was allowed to stand for 10–15 min so as to ensure full color development. Using distilled water as reference the red-violet to purple color formed was then measured at λ_{540} [17].

3. Results and discussion

3.1. Surface morphology and elemental composition study

Fig. 2 presents the surface structure and morphology of magnetic ferro photo gel before and after photocatalysis. It was clearly observed from the FESEM images that the surface of slice was rougher and appeared to have a shining appearance after photoreduction. This was probably due to the beads becoming increasingly covered with $Cr(OH)_3$.

EDX analysis was performed in conjunction with the FESEM analysis to determine the elemental composition of selected spots on magnetic bead surface. Table 1 exhibits the elemental compositions of magnetic bead before and after photoreduction.

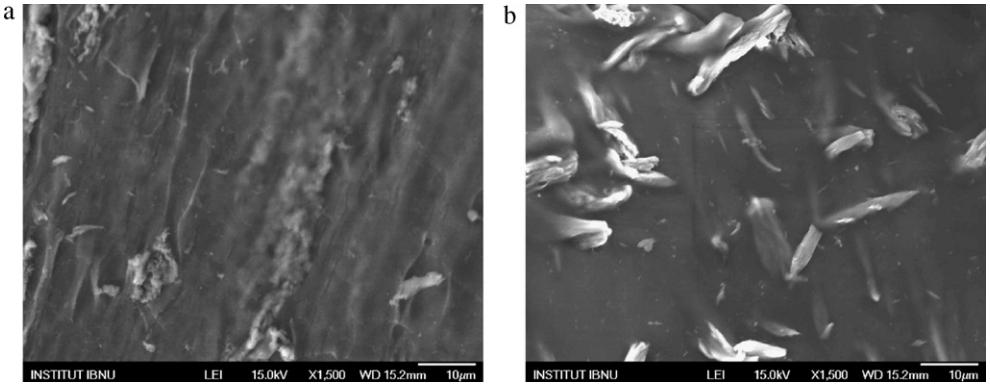

Fig. 2. FESEM images of magnetic beads: (a) before photoreduction and (b) after photoreduction.

Table 1
Mass percentage of the various elements on the magnetic photocatalyst beads before and after photoreduction.

Element	Mass percentage (%)	
	Before photoreduction	After photoreduction
Carbon	16.58	35.94
Oxygen	46.38	42.59
Sodium	0.34	0.00
Calcium	12.14	1.74
Chromium	0.00	0.54
Iron	24.20	18.93

It was observed that, besides Fe, Ca, and O, there were large amounts of residual carbon in the initial organic components. The results also indicated only small amounts of Cr were present on the surface after photoreduction and this could be explained in terms of absorption of Cr into magnetic beads. In general, anions adsorb through a ligand exchange reaction is favored at low pH, where the surface was positively charged and site hydration was favorable [5]. Considering γ-Fe_2O_3 has a positive charge at pH lower than the point of zero charge (pH_{zpc} = 7.3), it would be expected that the ionic form of Cr(III) ($Cr(OH)_3$) is deposited well on the magnetic beads surface.

3.2. Effect of initial concentration Cr(VI) on photoreduction kinetics

Fig. 3 illustrates the effect of initial concentration on the removal efficiency of Cr(VI). It was observed that the rate of Cr(VI) uptake was initially high, followed by a much slower subsequent removal rate leading gradually to an equilibrium condition. The rapid adsorption of Cr(VI) (40 min) by magnetic beads might be attributed to the surface adsorption process. Since nearly all the adsorption sites of the magnetic gels exist in the exterior and interior of the microporous gels, it was easy for the Cr(VI) to access these active sites, thus resulting in a rapid equilibration. Subsequently the Cr(VI) gets reduced to the stable Cr(III) form via direct reduction by the photoregenerated electrons and thus goes into solution giving way to more Cr(VI) to be attached to the adsorption sites. In comparison, the equilibration time for the photoreduction of Cr(VI) by some other catalyst was much longer. For instance, photoreduction of Cr(VI) by immobilized titania reach equilibrium after more than 30 h [7], while for the Cr(VI) uptake onto activated carbon is around 10–50 h [18]. At equilibrium, the removal efficiency of Cr(VI) at initial concentrations of 25, 50, 75, 100, 125 and 150 mg/L was found to be 100%, 100%, 100%, 100%, 70% and 70%, respectively. Furthermore, similar profile of the curves at each initial concentration indicated that the percentage adsorption of Cr(VI) decreased with

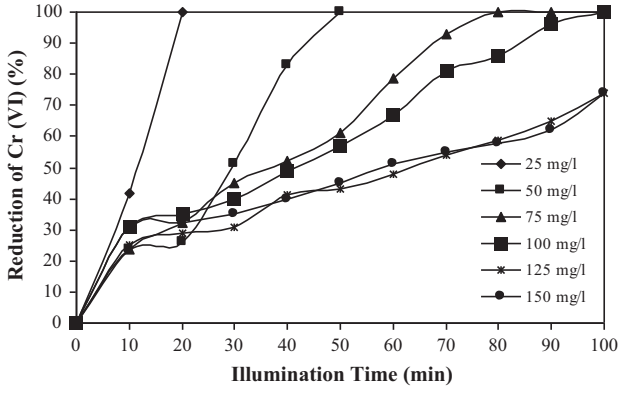

Fig. 3. Effect of time and initial concentration on photocatalytic reduction of Cr(VI) [catalyst dosage 16% (v/v); pH 1].

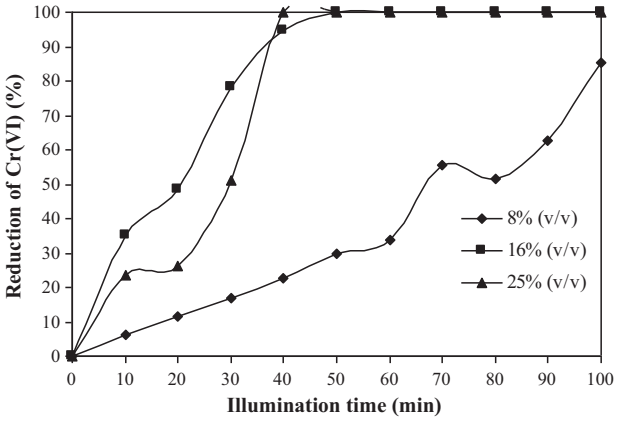

Fig. 4. Effect of catalyst concentration on photoreduction of Cr(VI) [initial Cr(VI) concentration is 50 mg/L; pH 1].

the increase in the initial Cr(VI) concentration. This was expected due to the fact that for a fixed adsorbent dosage, the total available adsorption sites were limited thus leading to a decrease in percentage removal of the adsorbate corresponding to an increased initial adsorbate concentration.

3.3. Effect of photocatalyst loading on the photoreduction of Cr(VI)

Photocatalyst dosage is another critical parameter to the photoreduction efficiency. In order to determine its effect on the reduction of chromium (VI), a series of experiments were conducted with varying catalyst concentrations from 8% to 25% (v/v). The results are illustrated in Fig. 4.

As the photocatalyst loading increased from 8% to 16% (v/v) the reduction efficiency of Cr(VI) was enhanced, and reached 100% after approximately 50 min treatment. The enhancement in the reduction efficiency of Cr(VI) was probably due to the increase in the catalyst amount which contributed to the increase in the active sites and number of photons adsorbed and thus increased chromium (VI) adsorption and reduction [4]. Apparently when the catalyst amount was further increased to 25% (v/v) not much change was observed in the reduction of Cr(VI). The 100% removal of Cr(VI) was observed at about 40 min. This was probably due to the blockage of sunlight caused by excessive catalyst loading. The results of the study seem to be in agreement with previous studies done by Mohapatra et al. [4] where they reported that the increase in the photocatalyst amount beyond the optimum dosage has a negative effect on the degradation efficiency. Light blocking by excessive catalyst may account for the decreased degradation efficiency. The excessive catalyst prevented the illumination of catalyst. In our case the rate of photo reduction did not enhance dramatically when the photocatalyst loading was increased beyond of 16% (v/v).

3.4. Kinetic modeling

Many researchers [5,19,20] have observed that the reduction rates of photocatalytic reduction and degradation of various inorganics over illuminated catalyst based metal oxide fitted the Langmuir–Hinshelwood (L–H) kinetics model. The Langmuir–Hinshelwood kinetic relates the rate of surface-catalysed reactions to the surface covered by the substrate. According to the L–H model, the rate of a unimolecular surface reaction is proportional to the surface coverage.

The surfaces of iron oxides are covered with hydroxyl groups whose forms vary at different pH [11]. The surface charge is neutral at pH_{zpc}. Below the pH_{zpc}, the adsorbent surface is positively

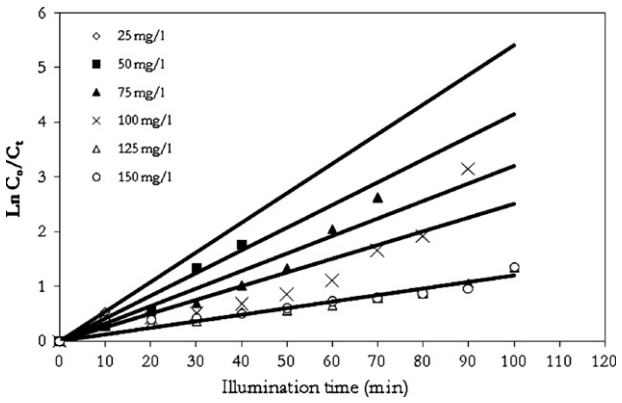

Fig. 5. Linear transform Ln $C_0/C_t = f(t)$ of the reduction of Cr(VI).

charged, and anion adsorption occurs. Since the surface of γ-Fe_2O_3 particles in aqueous solutions is covered with hydroxyl groups and water molecules, both Cr(VI), and water molecule (H_2O) could, in principle, be adsorbed on this surface via hydrogen bonds. Due to the competition for the same active sites which cannot be ignored, the (L–H) model needs to be expressed by [20]:

$$r = -\frac{dC}{dt} = k_r\theta = \frac{(k_r K_{LH} C)}{(1 + K_{LH}C + K_{H_2O}C_{H_2O})} \quad (1a)$$

where r is the photoreduction rate of the reactant (mg/L min), C the concentration of the reactant (mg/L), t is the illumination time, k_r is the reaction rate constant (mg/L min), K_{LH} is the adsorption coefficient of the reactant (L/mg), K_{H_2O} the solvent adsorption constant and C_{H_2O} the concentration of the water (Eq. (1a)). Since $C_{H_2O} \gg C$ and C_{H_2O} remains practically constant throughout the whole range of concentration, the part of the catalyst covered by water is fixed. In this section, all experimental conditions, such as pH, catalyst dosage, remained constant. Therefore, C will be the only variable in the initial reactions and can be expressed as follows [20]:

$$r = -\frac{dC}{dt} = \frac{k_r K_{LH} C}{1 + K_{LH}C} \quad (1b)$$

During photocatalytic reduction, due to the formation of intermediates, interference in the determination of kinetics may occur because of competitive adsorption and reduction. Thus, calculations were performed at the beginning illuminated conversion. During this period, any changes such as intermediates effects or pH changes can be neglected and the photocatalytic reduction rate expression as a function of the concentration is defined as:

$$r_0 = -\frac{dC}{dt} = k_r\left(\frac{K_{LH}C_0}{1 + K_{LH}C_0}\right) \quad (2)$$

where r_0 is the initial photocatalytic reduction rate (mg/L min) of chromium (VI) and C_0 the initial concentration of chromium (VI) (mg/L) and K_{LH} is the adsorption equilibrium constant (L/mg). In cases where the chemical concentration C_i is very low (C_0 small) the equation can be rearranged simply to an apparent first-order equation [21]

$$\mathrm{Ln}\left(\frac{C_0}{C_t}\right) = k_r K t = k_{app} t \quad (3)$$

where $k_r K = k_{app}$, C_t is the concentration of the chromium (VI) at time t, and C_0 is the initial concentration of the chromium (VI).

Generally, the initial reduction rate can be deduced as follows:

$$r_0 = k_{app} C_0 \quad (4)$$

A straight line is obtained when Ln (C_0/C_t) is plotted against time as depicted in Fig. 5. The apparent pseudo first-order rate constant k_{app} is represented by the slope of the line. The values obtained for the various initial concentrations are tabulated in Table 2.

Table 2
Pseudo-first order apparent constant values for Cr(VI) reduction.

Initial Cr(VI) concentration Co (mg/L)	Reaction rate, k_{app} (min^{-1})	R^2	Initial reaction rate, r_0 (mg/L min^{-1})
25	0.054	1.000	1.355
50	0.043	0.985	2.155
75	0.033	0.919	2.455
100	0.025	0.832	2.510
125	0.012	0.942	1.513
150	0.012	0.900	1.800

The following relationship is obtained when Eq. (2) is linearized:

$$\frac{1}{r_0} = \left(\frac{1}{k_r K_{LH}}\right)\left(\frac{1}{C_0}\right) + \frac{1}{k_r} \quad (5)$$

Based on the tabulated data in Table 2, $1/r_0$ is plotted against $1/C_0$. As illustrated in Fig. 6, $1/r_0$ correlates to $1/C_0$ well, thus the reduction of Cr(VI) by magnetic beads fitted with the Langmuir–Hinshelwood (L–H) kinetics model. According to the Langmuir–Hinshelwood (L–H) kinetics formula (Eq. (5)) fitted in Fig. 6, a straight line with an intercept of $1/k_r$ and a slope of $1/k_r K_{LH}$ is obtained, where k_r and K_{LH} are determined and the values are calculated to be 3.9 (mg/L min) and 0.0218 (L/mg) respectively. Correlation coefficient (R^2) for the regression line is 0.980. From the results obtained it was observed that $k_r > K_{LH}$, which suggested that a surface reaction, where the Cr(VI) was absorbed was the controlling step of the process. This finding is in line with other studies [5,20].

3.5. Regeneration of the beads

In order to use magnetic beads for industrial scale, it is necessary to make them attractive with regard to the usual methods of cleanup. Regeneration of loaded catalyst is a key factor in improving the economy of photocatalytic process. So, regeneration of loaded magnetic beads and metal recovery in a concentrated form are key factors for improving process economics. A successful desorption process must restore the catalyst close to its initial properties for effective reuse.

In this study the used magnetically separable photocatalyst beads were regenerated by treating them in 0.01 M NaOH for 1 h, after which they were used to treat Cr(VI) at initial concentrations of 25, 50, and 75 mg/L. The adsorbed Cr(VI) on the catalyst could be readily eluted and regenerated by 0.01 M NaOH solutions. The result was similar to the findings of Wang and Lo [13] who found

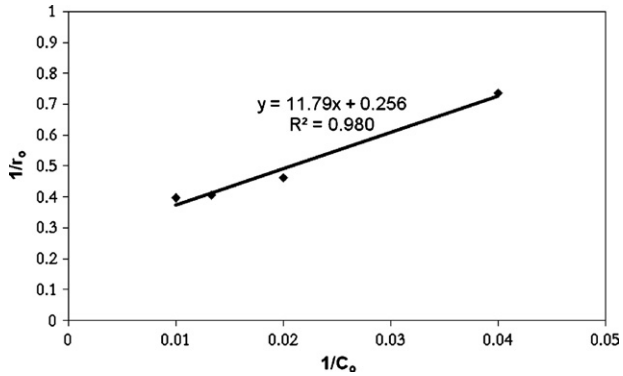

Fig. 6. The relationship between $1/r_0$ and $1/C_0$ at different initial concentrations of Cr(VI).

Table 3
Effect of usage time and regeneration of magnetic photocatalyst beads on Cr(VI) reduction at different initial Cr(VI) concentration 25, 50 and 75 mg/L performed at pH 1.

Time (min)	Reduction of Cr(VI) (%) at different initial Cr(VI) concentrations								
	25 mg/L			50 mg/L			75 mg/L		
	1st	2nd	3rd	1st	2nd	3rd	1st	2nd	3rd
0	0	0	0	0	0	0	0	0	0
20	67	60	32	58	19	13	26	9	8
40	100	98	50	96	50	17	40	23	9
60	100	100	70	100	88	32	60	47	20
80	100	100	92	100	100	52	82	62	30
100	100	100	100	100	100	73	100	92	40
120	100	100	100	100	100	88	100	94	55
140	100	100	100	100	100	100	100	100	65
160	100	100	100	100	100	100	100	100	80
180	100	100	100	100	100	100	100	100	100
200	100	100	100	100	100	100	100	100	100

that the used Fe_2O_3 could be regenerated by washing them with 0.01 M NaOH.

The potential of NaOH eluent could be explained on the basis of the system pH. The optimum pH for the Cr(VI) sorption was observed at pH 1 as reported in our previous work [11]. Hence, alkaline pH was unfavorable for Cr(VI) adsorption on catalyst surfaces and contrarily weakened the adsorption forces under such conditions. Thus, alkaline pH (13) facilitated the desorption of bound Cr(III) possibly via the formation of $Cr(OH)_4^-$.

The reduction results for the regenerated beads for different initial Cr(VI) are summarized in Table 3. The results were very encouraging because the photocatalyst activity could be partially regenerated by the regeneration process although the removal time was slightly increased. Complete removal of Cr (VI) using fresh magnetic photocatalyst beads took only 40 min and when the 1st regenerated bead are used again the removal rate remains almost unchanged for initial Cr(VI) of 25 mg/L. However when the magnetic photocatalyst beads were regenerated the 2nd time, complete Cr (VI) removal takes about 100 min. A similar trend is observed for the other initial Cr(VI) solutions. The results revealed that magnetic photocatalyst beads exhibited very good performances in the reduction of Cr(VI) in terms of their reusability and clearly suggested that the magnetic photocatalysts beads used in this study were quite stable for repeated use. In this case, the percentage of reduction was significant after being regenerated for the second time. However, after the 2nd regeneration, the magnetic beads have lost some of its original activity possibly because the magnetic particles leached out from the beads. If the alginate beads can be further strengthened these beads can be regenerated for the 3rd time and reused again.

4. Conclusion

The current investigation demonstrated that initial concentration of substrate and the catalyst greatly influenced the photoreduction of Cr(VI). It was found that the percentage adsorption of Cr(VI) decreased with the increase in the initial Cr(VI) concentration. This was expected due to the fact that for a fixed adsorbent dosage, the total available adsorption sites were limited thus leading to a decrease in percentage removal of the adsorbate corresponding to an increase initial adsorbate concentration. Moreover, the initial reaction rates were found to be directly proportional to catalyst concentration indicating the heterogeneous regime. However, it was observed that in excess of a critical concentration on the reaction rate decreased and become independent of the catalyst concentration. The photocatalytic reduction kinetics of Cr(VI) on magnetic beads is very much governed by the Langmuir–Hinshelwood kinetics model. The results, that $k_r > K_{LH}$, suggested that a surface reaction, where the Cr(VI) was absorbed, was the controlling step of the process. In addition the regenerated beads results were very promising since the photocatalyst activity could be restored by the regeneration process using NaOH and proved to be stable photocatalysts for repeated usage.

Acknowledgements

Financial support from the Ministry of Science, Technology and Environment through the FRGS fundings vote nos. 78404 and 78327 is gratefully acknowledged.

References

[1] F.C. Richard, A. Bourg, Aqueous geochemistry of chromium: a review, Water Res. 25 (1991) 807–816.
[2] H. Li, Z. Li, T. Liu, X. Xiao, Z. Peng, L. Deng, A novel technology for biosorption and recovery hexavalent chromium in wastewater by bio-functional magnetic beads, Bioresour. Technol. 99 (2008) 6271–6279.
[3] ATSDR, Draft Toxicological Profile for Chromium, US DHHS, Public Health Service, Atlanta, GA, 2008.
[4] P. Mohapatra, S.K. Samantaray, K. Parida, Photocatalytic reduction of hexavalent chromium in aqueous solution over sulphate modified titania, J. Photochem. Photobiol. A: Chem. 170 (2005) 189–194.
[5] J. Sun, X. Wang, J. Sun, R. Sun, S. Sun, L. Qiao, Photocatalytic degradation and kinetics of Orange G using nano-sized Sn(IV)/TiO_2/AC photocatalyst, J. Mol. Catal. A: Chem. 260 (2006) 241–246.
[6] D. Beydoun, R. Amal, G. Low, S. McEvoy, Role of nanoparticles in photocatalysis, J. Nanopart. Res. 1 (1999) 439–458.
[7] S. Tuprakay, W. Liengcharernsit, Lifetime and regeneration of immobilized titania for photocatalytic removal of aqueous hexavalent chromium, J. Hazard. Mater. B124 (2005) 53–58.
[8] M.F.J. Dijkstra, A. Michorius, H. Buwalda, H.J. Panneman, J.G.M. Winkelman, A.A.C.M. Beenackers, Comparison of the efficiency of immobilized and suspended systems in photocatalytic degradation, Catal. Today 66 (2001) 487–494.
[9] W. Qian, Q. Huijing, Y. Yueping, Z. Zhen, N. Cissoko, X. Xinhua, Reduction of hexavalent chromium by carboxymethyl cellulose-stabilized zero-valent iron nanoparticles, J. Contam. Hydrol. 114 (2010) 35–42.
[10] Y.P. Sun, X.Q. Li, W.X. Zhang, H. Paul Wang, A method for the preparation of stable dispersion of zero-valent iron nanoparticles, Colloids Surf. A. 308 (2007) 60–66.
[11] A. Idris, N. Hassan, N.S. Mohd Ismail, E. Misran, N. Yusuf, A.F. Ngomsik, A. Bee, Photocatalytic magnetic separable beads for chromium (VI) reduction, Water Res. 44 (2010) 1683–1688.
[12] J. Hu, I.M.C. Lo, G.H. Chen, Removal and recovery of Cr(VI) from wastewater by maghemite nanoparticles, Water Res. 39 (2005) 4528–4536.
[13] P. Wang, I.M.C. Lo, Synthesis of mesoporous magnetic γ-Fe_2O_3 and its application to Cr(VI) removal from contaminated water, Water Res. 43 (2009) 3727–3734.
[14] A.F. Ngomsik, A. Bee, J.M. Siaugue, V. Cabuil, G. Cote, Nickel adsorption by magnetic alginate microcapsules containing an extractant, Water Res. 40 (2006) 1848–1856.
[15] R.L. Pozzo, J.L. Giombi, M.A. Baltanas, A.E. Cassano, The performance in a fluidized bed reactor of photocatalysts immobilized onto inert supports, Catal. Today. 62 (2000) 175–187.
[16] N. Fauconnier, A. Bee, J. Roger, J.N. Pons, Synthesis of aqueous magnetic liquids by surface complexation of maghemite nanoparticles, J. Mol. Liq. 83 (1999) 233–242.
[17] Z.A. Zakaria, Z. Zakaria, S. Surif, W.A. Ahmad, Hexavalent chromium reduction by *Acinetobacter haemolyticus* isolated from heavy-metal contaminated wastewater, J. Hazard. Mater. 146 (2007) 30–38.

[18] S.B. Lalvani, A. Hubener, T.S. Wiltowski, Chromium adsorption by lignin, Energy Sources 22 (2000) 45–56.
[19] M.H. Khedr, K.S. Abdel Halim, N.K. Soliman, Synthesis photocatalytic activity of nano-sized iron oxides, Mater. Lett. 63 (2009) 598–601.
[20] N. Guettai, H. Ait Amar, Photocatalytic oxidation of methyl orange in presence of titanium dioxide in aqueous suspension. Part II. Kinetics study, Desalination 185 (2005) 439–448.
[21] D. Chen, A.K. Ray, Photocatalytic kinetics of phenol and its derivatives over UV irradiated TiO_2, Appl. Catal. B: Environ. 23 (1999) 143–157.